Chemosphere 89 (2012) 172–178

Contents lists available at SciVerse ScienceDirect

Chemosphere

journal homepage: www.elsevier.com/locate/chemosphere

Electrochemical removal of nitrate using ZVI packed bed bipolar electrolytic cell

Joo-Young Jeong, Han-Ki Kim, Jung-Hwan Kim, Joo-Yang Park *

Department of Civil and Environmental Engineering, Hanyang University, 17 Haengdang-dong, Seongdong-gu, Seoul 133-791, Republic of Korea

HIGHLIGHTS

- The packing ratio of 1:1 and 2:1 (sand:ZVI) showed better current efficiency.
- The feed flow rate of 30 mL min^{-1} showed optimum current efficiency.
- Effluent pH was proportional to nitrate influx concentration.
- The nitrate was converted to ammonia as final product of nitrate reduction.
- The magnetite was found on the surfaces as corrosion products of ZVI.

ARTICLE INFO

Article history:
Received 4 January 2012
Received in revised form 15 May 2012
Accepted 16 May 2012
Available online 25 June 2012

Keywords:
Bipolar electrolytic cell
Nitrate removal
Zero valent iron
Magnetite

ABSTRACT

The present study investigates the performance of the zero valent iron (ZVI, Fe^0) packed bed bipolar electrolytic cell for nitrate removal. The packing mixture consists of ZVI as electronically conducting material and silica sand as non-conducting material between main cathode and anode electrodes. In the continuous column experiments for the simulated groundwater (initial nitrate and electrical conductivity of about 30 mg L^{-1} as N and 300 μS cm^{-1}, respectively), above 99% of nitrate was removed at the applied potential of 600 V with the main anode placed on the bottom of reactor. The influx nitrate was converted to ammonia (20% to maximum 60%) and nitrite (always less than 0.5 mg L^{-1} as N in the effluent). The optimum packing ratio (v/v) of silica sand to ZVI was found to be 1:1–2:1. Magnetite was observed on the surface of the used ZVI as corrosion product. The reduction at the lower part of the reactor in acidic condition and adsorption at the upper part of the reactor in alkaline condition are the major mechanism of nitrate removal.

1. Introduction

Nitrate contamination in groundwater has become an ever-increasing and serious environmental problem since 1970s. The excessive application of fertilizers in agriculture causes the infiltration of large quantities of nitrate into underground and surface water (Zhou et al., 2007). The international drinking water quality standards recommended 50–100 mg L^{-1} as an acceptable level for nitrate (Koparal and Öütveren, 2002; Choi et al., 2009) and the maximum contaminant level (MCL) was set by EPA for nitrate of 10 mg L^{-1} as N. Nitrate is very difficult to be removed by precipitation and adsorption because it is seldom complexed with cations. Conventional drinking water purification processes including flocculation, sedimentation and filtration appear to show no measurable effects for nitrate removal (Paidar et al., 2002; Zhou et al., 2007). Physical and chemical methods such as reverse osmosis, chemical denitrification and electrodialysis have been developed for elimination of nitrate from water (Follett and Hatfield, 2001). However, these nitrate removal processes have various limitations and are particularly not suitable for small communities that suffer nitrate contamination of the groundwater of their wells. To overcome these problems, electrochemical technologies have become studied for the removal of nitrate (Lacasa et al., 2011). Electrochemical methods through the selective nitrate reaction have several advantages: no requirement of chemicals before and after the treatment, production of the fewer amounts of sludge, small area demand and low investment cost (Koparal and Öütveren, 2002). The electrokinetic method is applicable to any electrically charged organic or inorganic species in water. In the electric field, positively charged ions migrate towards the cathode and negatively charged ions migrate towards the anode. The nitrate was attracted towards and concentrated near the anode in the electrical field and it would even retain nitrates with artificial flow (Eid et al., 1999). When the potential is applied, reactions (1) and (2) take place at the anode and cathode with electrolysis of water. If the produced ions are neither removed nor neutralized with other chemical reaction, these reactions lower the pH at the anode and raise it at the cathode (Probstein and Hicks, 1993):

* Corresponding author. Tel.: +82 2 2220 0411; fax: +82 2 2220 1945.
E-mail address: jooypark@hanyang.ac.kr (J.-Y. Park).

0045-6535/$ - see front matter © 2012 Elsevier Ltd. All rights reserved.
http://dx.doi.org/10.1016/j.chemosphere.2012.05.104

$$2H_2O + 2e^- \rightarrow H_{2(g)} + 2OH^- \quad (1)$$

$$2H_2O \rightarrow O_{2(g)} + 4H^+ + 4e^- \quad (2)$$

For electrolysis, there are two different electrode configurations, namely monopolar and bipolar. In the monopolar mode, all the electrodes are alternately tapped by electricity, whereas in the bipolar mode, only the electrodes at both ends are connected to electricity. Bipolar electrodes have been used in industrial reactors for applications such as electrosynthesis and water splitting and also for increasing fuel cell performances (Loget and Kuhn, 2011). The advantages of bipolar electrolysis are that it can pack as many as electrodes in a given space and the ohmic drop is low since the cathode and anode are located in the vicinity. However, these electrodes are limited in operating life because the structure finally agglomerates into a solid mass and clogs of the bed (Hadžismajlović et al., 1996). For efficient bipolar electrolysis, the electrolyte solution should have low electrical conductivity (Juvekar et al., 2009).

In this study, nitrate in a simulated groundwater was treated by the electrochemical method using ZVI packed bed bipolar electrolytic cell. Characteristics of electrolysis were investigated using multiple continuous experiments to find out the better operation parameters such as electrode position, packing ratio and flow rate (retention time). Performance of these reactors was also discussed with electric current consumption and reaction products of ZVI.

2. Materials and methods

2.1. Set-up and procedure

The electrolytic cell is composed of a number of electro-conductive particles packed between two main electrodes, and each particle works as an electrode. ZVI was used not only as conductive particles but also as an electron donor. The silica sand was used as non-conductive particle because it unlikely interferes with the nitrate reduction by ZVI (Huang and Zhang, 2005). Fig. 1 shows the schematic diagram of ZVI packed bed bipolar electrolytic cell.

Table 1
The properties of simulated groundwater (based on the compositions of the groundwater in stock farming community).

Parameter	Value
pH	6.8–8.0
Electrical conductivity	249–369 μS cm^{-1}
Nitrate	28.5–32.2 mg L^{-1} as N
Temperature	17.3–25.1 °C

The reactor was made of a cylindrical acrylic resin (8 cm inner diameter, 20 cm height), and the bed volume was 1 L (HRT was 36 min at flow rate of 10 mL min^{-1}). The cathode was placed on the top and the anode was placed on the bottom of the reactor with cork gaskets for keeping water tightness between flanges. To achieve uniform flow in the reactor, the feed solution was injected in upward direction by using a peristaltic pump. To improve flow distribution, spherical glass beads (5 mm diameter) were packed at the bottom of reactor. The simulated groundwater was synthesized based on the compositions of the groundwater in a small community that are polluted with nitrate about 30 mg L^{-1} as N due to stock farming. The main characteristics of simulated groundwater are given in Table 1. All aqueous solutions were prepared using deionized water. The porosity of the silica sand-ZVI mixture bed was measured to be 36%.

2.2. Chemicals and materials

Sodium nitrate ($NaNO_3$ > 99.0%, guaranteed reagent, Junsei) and sodium chloride (NaCl > 99.0%, ACS reagent, Sigma–Aldrich Inc., USA) as electrical conductivity adjustment were used for making simulated groundwater contaminated with nitrate. A peristaltic pump (Easy-load® II, Cole-Parmer Instrument Co.) and tubing (4.8 mm inner diameter, 96410-25, Masterflex®) were used to feed the solution uniformly. Sphere type of ZVI (Fe > 98.4%, 0.6 mm diameter, Sanga Co.) and silica sand (<0.3 mm diameter, Joomoonjin silica sand Co.) were used as packing materials (780 g of silica sand and 1340 g of ZVI were used for each experiment). Direct

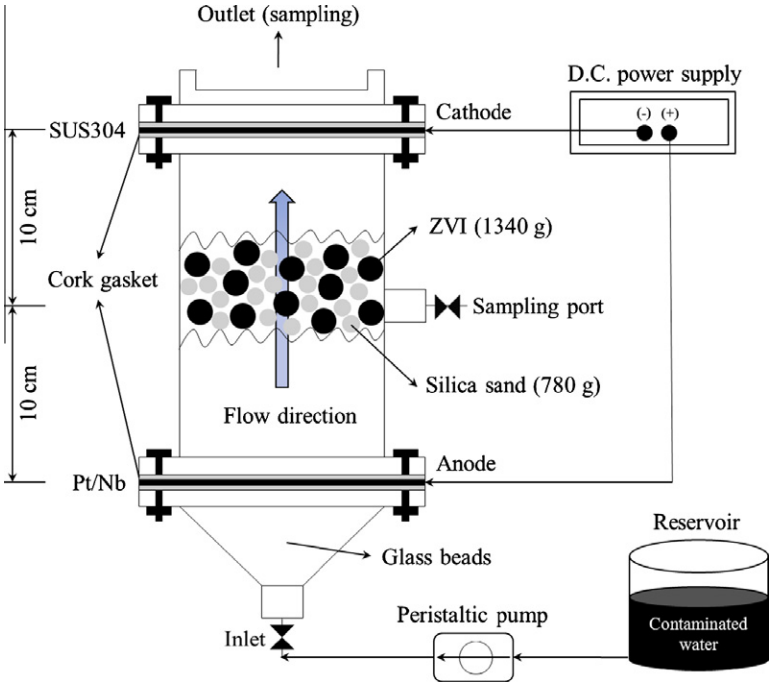

Fig. 1. The schematic diagram of ZVI packed bed bipolar electrolytic cell (not to scale) (reactor volume, 1 L; porosity, 36%; HRT, 36 min at flow rate 10 mL min^{-1}).

current (DC) power supply (XG600-2.8, Sorensen) was used to apply potential 600 V to the reactor and to check the electric current consumption. The nitrate removal kinetics was faster in the higher voltage; however the voltage was determined 600 V because voltage could not elevate unlimitedly. Adequate safety precautions were taken with respect to power supply. Platinum clad niobium netting was used as an anode to avoid sacrificial anode and stainless steel netting was used as a cathode (an electrode gap of 200 mm).

2.3. Analytical methods

In all experiment, all samples obtained at the top of reactor unless otherwise specifically stated were analyzed after filtration with 0.45 μm syringe filter. Nitrate, nitrite and ammonia were measured by a HACH model DR-2800 spectrophotometer (APHA, 1998). To observe the particle size and morphological surface changes, field emission scanning electron microscope (FESEM, SUPRA 55VP, Carl Zeiss) was used at 2 kV of acceleration voltage. X-ray diffraction (XRD) was performed on a Bruker AXS D8 Advance (Cu Kα source, 40 kV, 40 mA) and analyzed with the EVA software. The diffraction was measured between 2θ angle of 5–80° with step size of 0.06° and scan rate was 2° min^{-1}.

Current efficiency was calculated by Faraday's law of electrolysis as shown in the following equation:

$$\text{Effective current}(I_E) = \frac{(C_{in} - C_{out}) \times z \times V \times F}{t \times M} \quad (3)$$

$$\text{Currentefficiency} = \frac{I_E}{I} \times 100 \quad (4)$$

where C_{in} and C_{out} are the input and output concentration after time t of nitrate (mg L^{-1} as N), z is the valency number of ions of the substance, V is the 1 pore volume of reactor (L), F = 96,485 C mol^{-1} is the Faraday constant, t is the total electrolysis time with 1 pore volume (s), M is the molar mass of the substance (g mol^{-1}) and I is the actual current applied at the reactor (A). When the current efficiency was calculated based on measured current, it can be lower than the theoretical value because the value does not consider the electrolysis of water.

3. Results and discussion

3.1. Effect of main electrode configuration

Fig. 2 shows the removal efficiency (C/C_0) and pH of samples taken at the middle and the top of the reactor from two different configurations of main electrodes: (a) main anode net and (b) main cathode net at the bottom of reactor with packing ratio 2:1 (silica sand:ZVI), flow rate 10 mL min^{-1}, initial nitrate concentration 30 mg L^{-1} and 600 V. The maximum removal rate of 95% at the top of the reactor was observed in case that the anode net was placed at the bottom of the reactor. In this case, pH has risen to 10.4 at the middle of reactor and 11.0 at the top of reactor. The pH rose seems due to consumption of hydrogen ions during the nitrate reduction with iron corrosion as described in Eqs. (5)–(9). Almost all of nitrate was removed after 2 h before passing the middle part of the reactor. This indicates that the anode placed at the bottom of reactor made the ZVI particles under the middle point corroded to provide a suitable environment for reduction of nitrate. A slight pH increase from middle to top is due to the cathodic action described in Eq. (1):

$$NO_3^- + Fe^0 + 2H^+ \rightarrow Fe^2 + + H_2O + NO_2^- \quad (5)$$

$$NO_3^- + 4Fe^0 + 10H^+ \rightarrow 4Fe^{2+} + NH_4^+ + 3H_2O \quad (6)$$

$$2NO_3^- + 5Fe^0 + 12H^+ \rightarrow 5Fe^{2+} + N_{2\,(g)} + 6H_2O \quad (7)$$

$$NO_2^- + 3Fe^0 + 8H^+ \rightarrow 3Fe^{2+} + NH_4^+ + 2H_2O \quad (8)$$

$$2NO_2^- + 3Fe^0 + 8H^+ \rightarrow 3Fe^{2+} + N_{2\,(g)} + 4H_2O \quad (9)$$

On the contrary, when the cathode was placed at the bottom of the reactor, nitrate was not nearly removed up to the middle of the reactor and only 55% of nitrate was removed from the middle to the top. At this configuration of main electrodes, the cathode at the bottom nearly could not corrode the ZVI particles under the middle point. The reductive reactions of nitrate described in Eqs. (5)–(9) could not be proceeded without corrosion of ZVI. The cathode net and the ZVI bipolar electrodes under the middle point merely reduced water to produce hydroxide ions as shown in Eq. (1), thereby increasing the pH to around 11. The ZVI particles near the top of the reactor could be corroded by the anode net placed on the top but not as much as at the other configuration. So nitrate was reduced as much lower at this configuration. The pH was decreased to 8.7 at the top after 3 h because the anode net and nearby ZVI bipolar electrodes partially oxidized water to produce protons as described in Eq. (2). The corrosion of iron particles seems to be an important step for efficient reduction of nitrate in this bipolar cell. Therefore it can be concluded that placing anode at the bottom was much more effective for reduction of nitrate than placing cathode at the bottom because the former configuration could corrode ZVI particles more efficiently.

3.2. Effect of packing ratio

Fig. 3 shows the removal efficiency (C/C_0) and pH (a), temperature (b), current (c) and current efficiency (d) at different packing ratios of silica sand to ZVI. Bipolar reactors with five different packing ratios (v/v) of silica sand to ZVI (silica sand only, 4:1, 2:1, 1:1, and 1:2) were examined to determine the optimal packing ratio (flow rate 10 mL min^{-1} and 600 V). When the simulated groundwater with nitrate of 30 mg L^{-1} as N was injected into the reactor from bottom, maximum removal efficiency of 84% was obtained in the packing ratio 1:2 (silica sand to ZVI) at 40 min (Fig. 3a), and the maximum current efficiency of 16% was obtained in the 1:1 at 60 min (Fig. 3d). At the later stage of the operation, removal efficiency for all packing ratios was almost converged to around 70%. Initial kinetic of nitrate removal was faster but the electricity consumption was higher at the higher content of ZVI in the mixture (in case of 1:2 Fig. 3c). Reactors with no ZVI, operated at the monopolar mode, showing similar kinetics of nitrate removal at the initial stage but with very high temperature and high electricity consumption. At this time, the reaction will occur at the main electrode. However, it does not facilitate electron transfer because it will not have enough electrolytes in the solution and, electrode gap is wide. Thus, efficiency will drop although high voltage is applied because of electrolysis of water. Further operation could not be proceeded due to excessively violent reaction. In all cases, the nitrite was less than 0.5 mg L^{-1} as N and the ferrous iron was measured around 1 mg L^{-1} in effluent. Based on the results of this experiment, the packing ratio between 1:1 and 2:1 was determined as the optimum ratio because higher current efficiency was observed. At these ratios, each ZVI particle was well separated which were present to maximize the contact area between nitrate and ZVI and an individual particle acted more like a tiny electrolytic cell than 4:1 or 1:2 ratios.

3.3. Effect of inflow nitrate concentration on effluent pH

By positioning the cathode at the top of the reactor, pH value of the effluent was 9.5–10.0 due to hydroxide ions generated by elec-

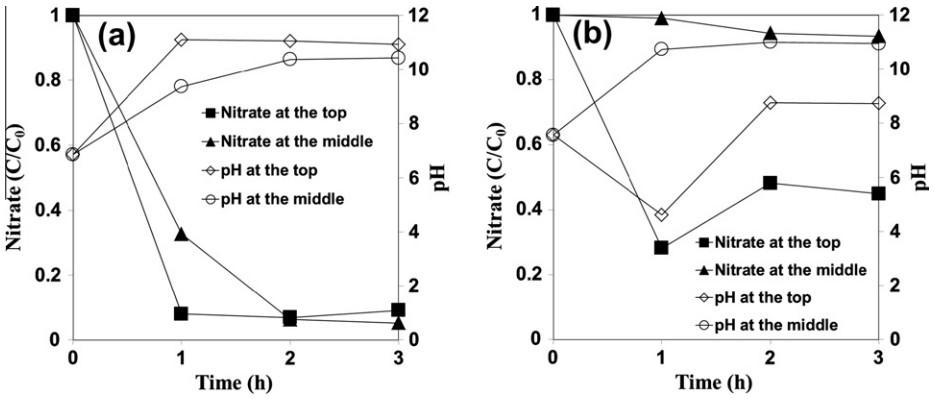

Fig. 2. The removal efficiency (C/C_0) of nitrate and pH with different electrode position, anode at the bottom (a) and cathode at the bottom (b) (initial concentration, 30 mg L^{-1} as N; packing ratio, 2:1; potential, 600 V; flow rate, 10 mL min^{-1}).

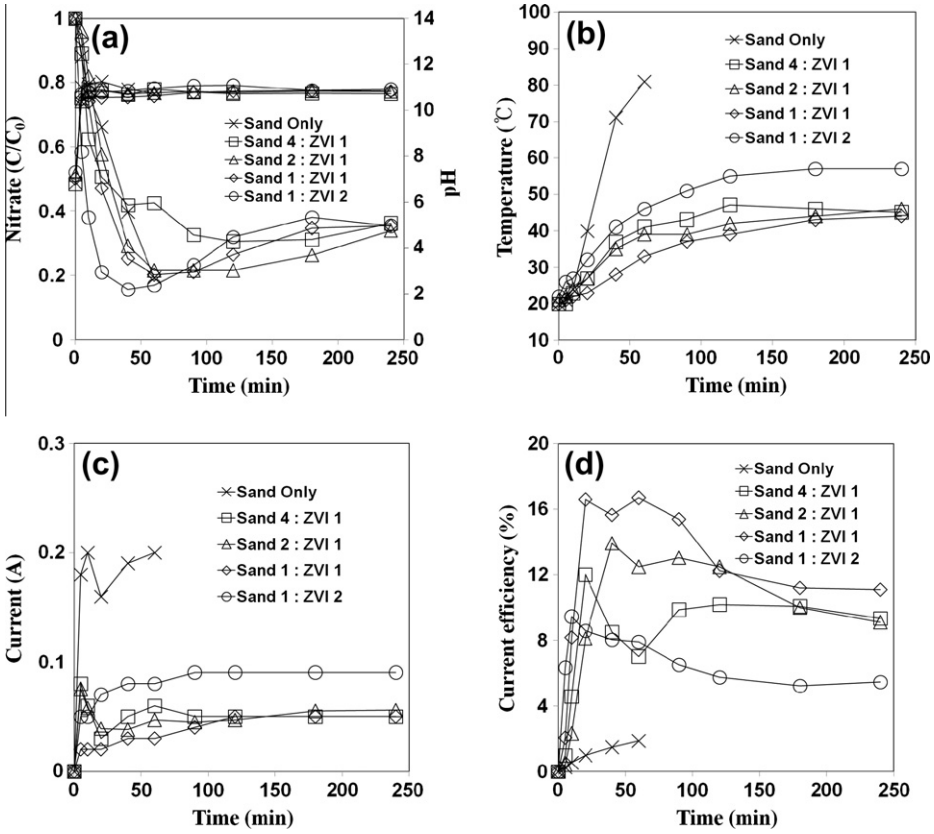

Fig. 3. The removal efficiency (C/C_0) and pH (a), temperature (b), current (c), and current efficiency (d) with different packing ratios (initial concentration, 30 mg L^{-1} as N; potential, 600 V; flow rate, 10 mL min^{-1}).

trolysis when no nitrate was added to the reactor. The pH was about 10.8 when nitrate was added at the concentration of 30 mg L^{-1} as N. Although the results of other influent concentrations which are not presented in figures, when the simulated groundwater contained nitrate of 90 mg L^{-1} and 270 mg L^{-1} as N, the pH values of the effluent were about 11.2 and 11.6, respectively at the packing ratio of 2:1 (silica sand to ZVI), flow rate of 10 mL min^{-1} and 600 V. The removal efficiency at 40 min was 92% and 88%, respectively. The reduction of nitrate that mediated by oxidation of ZVI as shown in Eqs. (10)–(12) produced hydroxide ions of which the amount was stoichiometrically increased with the increase of the input concentration of nitrate. Thereby the pH as well as the current was proportionally increased with addition of more nitrate into the reactor due to the effect of increased electrolyte. Thus, the increased electric current will cause the increase of temperature.

$$6NO_3^- + 10Fe^0 + 3H_2O \rightarrow 5Fe_2O_3 + 6OH^- + 3N_{2\,(g)} \quad (10)$$

$$2NO_3^- + 5Fe^0 + 6H_2O \rightarrow 5Fe^{2+} + N_{2\,(g)} + 12OH^- \quad (11)$$

$$NO_3^- + 4Fe^0 + 7H_2O \rightarrow 4Fe^{2+} + NH_4^+ + 10OH^- \quad (12)$$

3.4. Effect of loading rate

To examine the capacity of the reactor in removing nitrate, input flow rates were increased gradually (10, 20, 30 and 40 mL min^{-1}) at

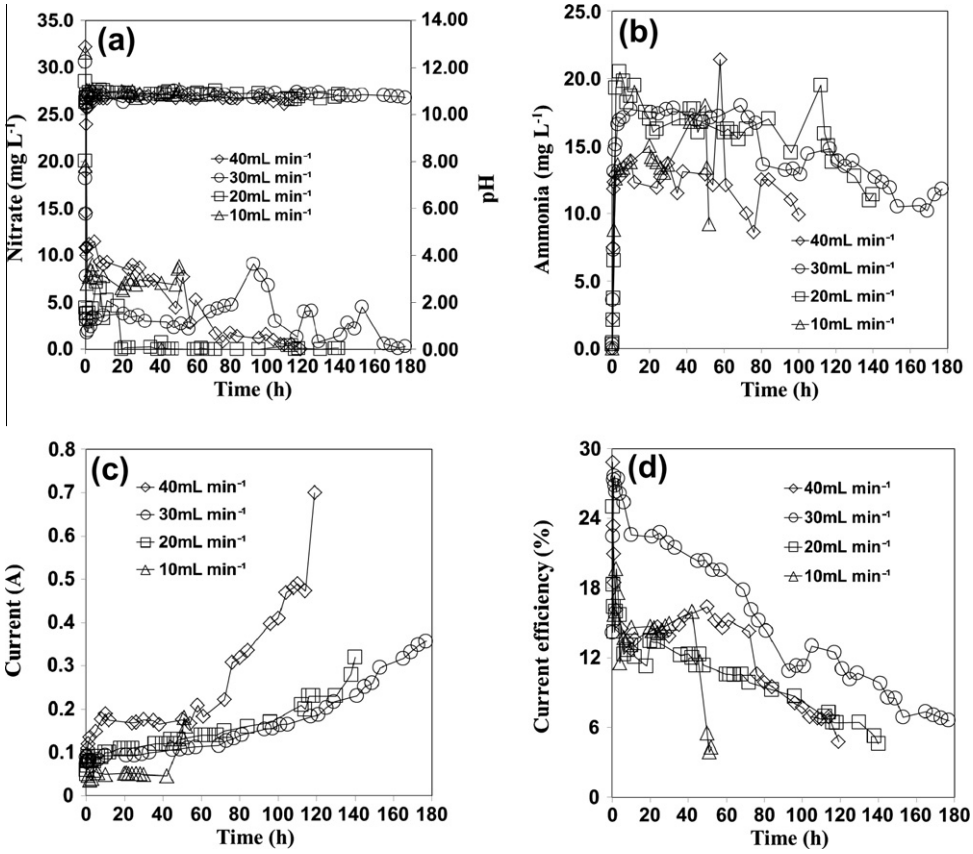

Fig. 4. The removal of residual nitrate and pH (a), ammonia in effluent (b), current (c), and current efficiency (d) at different flow rates (initial concentration, 30 mg L^{-1} as N; potential, 600 V; packing ratio, 2:1).

the packing ratio 2:1 and 600 V. Fig. 4 shows the variation of residual nitrate and pH (a), ammonia in effluent (b), current (c) and current efficiency (d) over time at different flow rates. The pH was maintained 10.7–10.8 at effluent in all experiments (Fig. 4a) and current increased with the lapse of time (Fig. 4c). Higher feed of the simulated groundwater at the normal temperature was expected to cool the generated heat in the reactor more efficiently. However, higher feed also loads more nitrates and electrolytes to the reactor, thereby generating more heat with increase of bypass current. For these reasons, there exists an optimal value of the feed flow rate. The reactor had been operated for all cases until the temperature reached 80 °C because the operation above the temperature could not be continued due to turbulent conditions generated by excess amount of gas bubbles and heat. The optimal flow rate was determined to be 30 mL min^{-1}. At this flow rate, nitrate was consistently removed below 10 mg L^{-1} as N, and current efficiency was the highest among them (Fig. 4d). At the flow rate of 40 mL min^{-1}, nitrate was removed similarly but current and temperature were increased sharply. The removal efficiencies of all reactors was gradually increased. The maximum removal efficiency was observed to be 99% at 20 mL min^{-1}. The gradual increase of removal efficiencies should be an outcome of elevated temperature since kinetics of nitrate reduction is accelerated by temperature increase (Ginner et al., 2004).

3.5. Examination of used ZVI particles

Fig. 5 shows the FESEM of the original surfaces of ZVI (Fig. 5a) and the used ZVI that were sampled from the upper part of the reactor after completion of the previous (at flow rate 20 mL min^{-1}) experiment. This analysis observed a disk like structure (Fig. 5b) and iron oxides having crystal (Fig. 5c) and spherical structure (Fig. 5d). Magnetite (Fe_3O_4), lepidocrocite (γ-FeOOH), maghemite (γ-Fe_2O_3), hematite (α-Fe_2O_3) and green rust (mixed valence Fe^{II}–Fe^{III} hydroxyl salts) are known as the major corrosion products of ZVI (Huang and Zhang, 2005). According to the XRD result of Fig. 5e, magnetite seems to be the major corrosion product in this system, and other researchers have also reported magnetite as corrosion product (Krajangpan et al., 2008; Kassaee et al., 2011). Aqueous ferrous ion and its precipitate such as iron (II) hydroxide might promote the formation of magnetite coated onto the surface of iron grains, which would greatly enhance transformation of nitrate to ammonium and nitrogen gas as described by the Eqs. (13) and (14) (Huang and Zhang, 2005; Correa et al., 2006).

$$NO_3^- + 2.82Fe^0 + 0.75Fe^{2+} + 2.25H_2O \rightarrow NH_4^+ + 1.19Fe_3O_{4\,(s)} + 0.5OH^- \quad (13)$$

$$15Fe(OH)_{2\,(s)} + 2NO_3^- \rightarrow 5Fe_3O_{4\,(s)} + N_{2\,(g)} + 2OH^- + 14H_2O \quad (14)$$

Nitrite, nitrogen gas and ammonia are possible products of the nitrate reduction as described in Eq. (5)–(14) (Chew and Zhang, 1999; Kassaee et al., 2011; Zhang et al., 2011). Nitrite derived by reduction of nitrate can cause disease and various health disorders such as birth defects. Nitrate was converted to nitrite in the first stage. But fortunately, nitrite is rapidly consumed upon further electrolysis (Peel et al., 2003). Above all, ammonia and nitrogen gas were known as the end products of nitrate reduction (Huang et al., 1998; Chew and Zhang, 1999). In all experiments, the influx nitrate was converted to ammonia of 20% to maximum 60%, and the conversion rate showed a decreasing tendency over time (Fig. 4b). Such a low conversion rate is mainly due to stripping of

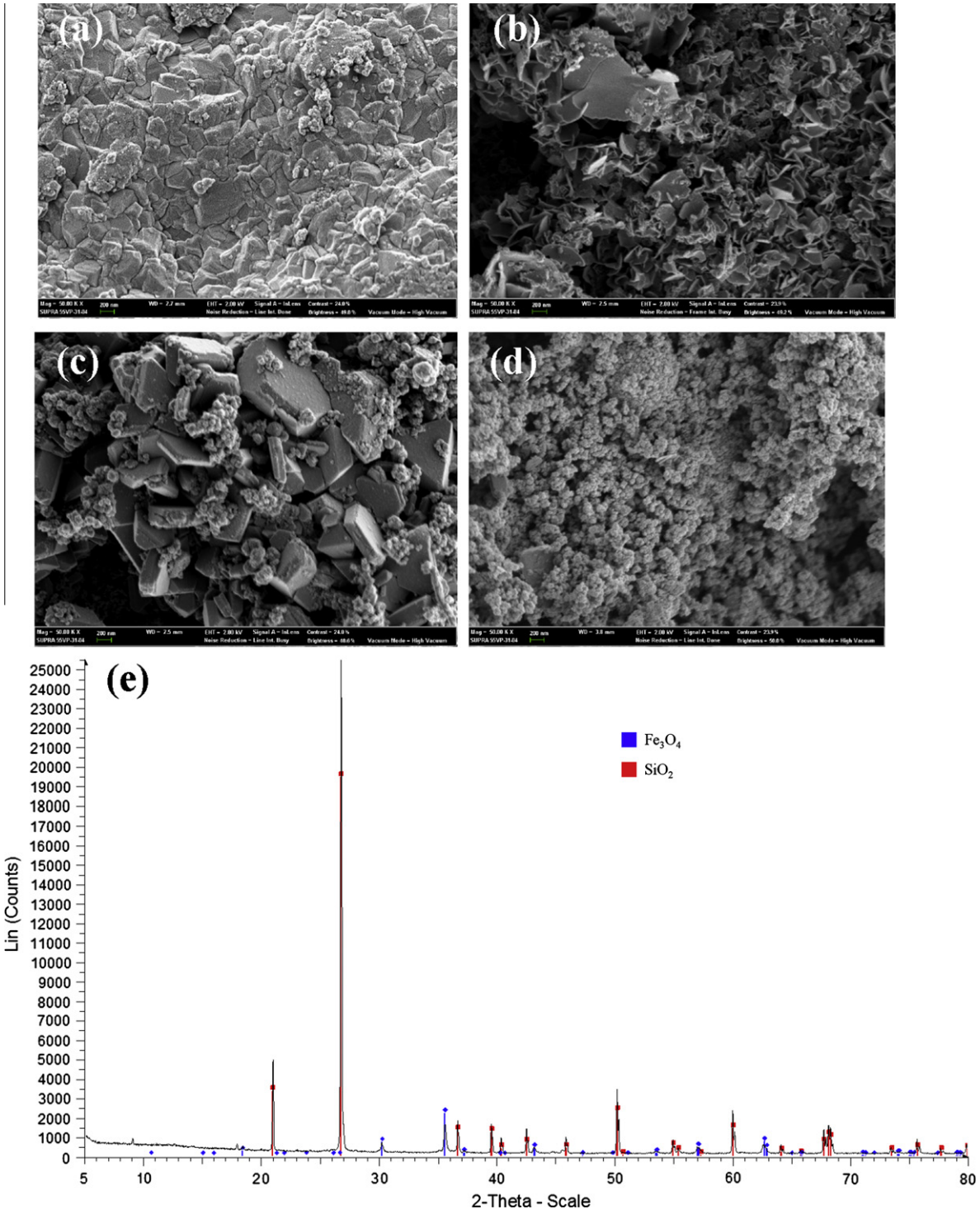

Fig. 5. The FESEM micrograph of iron surface with magnification 50 K: original surface of ZVI (a), disk like structure (b), crystal (c), and spherical structure (d). XRD pattern of the oxidized ZVI (e).

ammonia at high pH and temperature. Direct adsorption of nitrate on corrosion products of ZVI also might be a minor reason for lower ammonia recovery.

3.6. Nitrate removal mechanism

The removal mechanism of nitrate in this system is illustrated in Fig. 6. When the simulated groundwater was passing through the anode in the bottom of reactor, transportation of nitrate to cathode could be retarded due to the electrical migration and then nitrate could be reduced more easily by the generated electrons in the regions near anode. Furthermore, acidic environment near the anode due to generated hydrogen ions with electrolysis of water can accelerate the corrosion of iron, whereupon nitrate reduction also would be accelerated. Extending the range of acidic environment from the bottom of the reactor is able to hinder formation of iron oxides. It extends the operation time and increases the active surface of ZVI particles. As the flow progresses, the upper

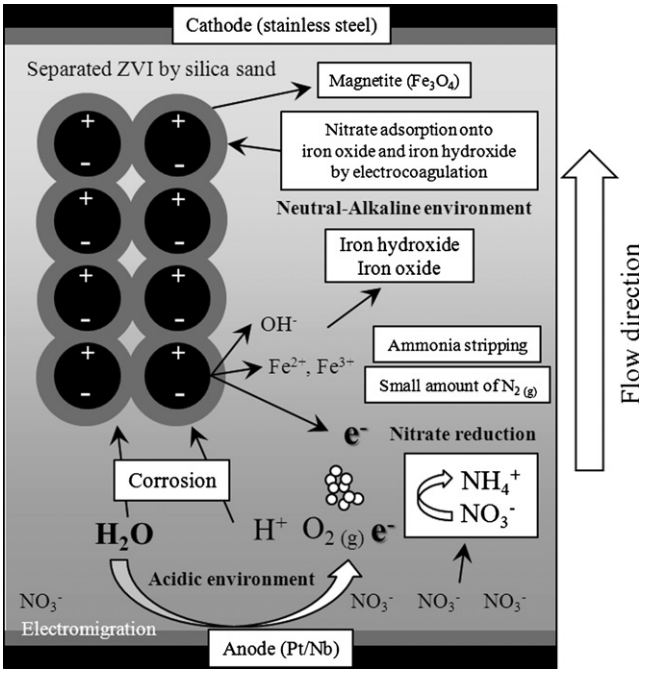

Fig. 6. Illustration of nitrate removal mechanism for electrolytic cell.

part of the reactor gradually becomes alkaline with reaction of iron. Under these pH conditions, the nitrate is removed by adsorption onto the iron oxide and hydroxide with electrocoagulation process. The ferrous ion generated by corrosion of ZVI can take many forms of magnetite and other oxide during passing through the cathode, which might remove a small amount of nitrate by adsorption (Hsia et al., 1994). Also, a part of ammonia generated by nitrate reduction process is stripped by generated oxygen gas at anode.

4. Conclusions

Placing anode at the bottom was much more effective for reduction of nitrate than placing cathode at the bottom because the former could corrode ZVI particles more efficiently. The reactor of the packing ratio of 1:1 and 2:1 (silica sand:ZVI) showed better current efficiency. At higher ratio of ZVI in a mixture, fast initial kinetic was observed but current efficiency was decreased due to high current. The feed flow rate of 30 mL min^{-1} showed optimum current efficiency which means that maximum nitrate was removed at consumption of minimum current. Effluent pH was proportional to nitrate influx concentration. Ammonia which is the final product of nitrate reduction was 20% to maximum 60% of nitrate influx and magnetite was found on the surfaces as corrosion products of ZVI. Thus the ZVI packed bed reactor at which anode is placed at the bottom with upward flow seemed to be suitable for the treatment of anionic pollutant that is removable by reduction and adsorption, especially with low concentration.

Acknowledgements

The financial support of this research by the Commercialization of Patented Technologies Program of Seoul Business Agency is gratefully acknowledged (Grant No. PA100095).

References

APHA, 1998. Standard Methods for the Examination of Water and Wastewater, 20th Ed. American Public Health Association, Washington, DC.
Chew, C.F., Zhang, T.C., 1999. Abiotic degradation of nitrates using zero-valent iron and electrokinetic processes. Environ. Eng. Sci. 16, 389–401.
Choi, J.H., Maruthamuthu, S., Lee, H.G., Ha, T.H., Bae, J.H., 2009. Nitrate removal by electro-bioremediation technology in Korean soil. J. Hazard. Mater. 168, 1208–1216.
Correa, J.R., Canetti, D., Castillo, R., Llópiz, J.C., Dufour, J., 2006. Influence of the precipitation pH of magnetite in the oxidation process to maghemite. Mater. Res. Bull. 41, 703–713.
Eid, N., Larson, D., Slack, D., Kiousis, P., 1999. Nitrate electromigration in sandy soil in the presence of hydraulic flow. J. Irrig. Drain. Eng. 125, 7–11.
Follett, R.F., Hatfield, J.L., 2001. Nitrogen in the environment: sources, problems, and management. TheScientificWorldJournal 1, 920–926.
Ginner, J.L., Alvarez, P.J.J., Smith, S.L., Scherer, M.M., 2004. Nitrate and nitrite reduction by Fe^0: influence of mass transport, temperature, and denitrifying microbes. Environ. Eng. Sci. 21, 219–229.
Hadžismajlović, D.E., Popov, K.I., Pavlović, M.G., 1996. The visualization of the electrochemical behaviour of metal particles in spouted, fluidized and packed beds. Powder Technol. 86, 145–148.
Hsia, T.H., Lo, S.L., Lin, C.F., Lee, D.Y., 1994. Characterization of arsenate adsorption on hydrous iron oxide using chemical and physical methods. Colloids Surf. A 85, 1–7.
Huang, Y.H., Zhang, T.C., 2005. Enhancement of nitrate reduction in Fe^0 – packed columns by selected cations. J. Environ. Eng. 131, 603–611.
Huang, C.P., Wang, H.W., Chiu, P.C., 1998. Nitrate reduction by metallic iron. Water Res. 32, 2257–2264.
Juvekar, V.A., Patil, R.S., Gurumoorthy, A.V.P., Contractor, A.Q., 2009. Analysis of multiple reactions on a bipolar electrode. Ind. Eng. Chem. Res. 48, 9441–9456.
Kassaee, M.Z., Motamedi, E., Mikhak, A., Rahnemaie, R., 2011. Nitrate removal from water using iron nanoparticles produced by arc discharge vs. reduction. Chem. Eng. J. 166, 490–495.
Koparal, A.S., Öütveren, U.B., 2002. Removal of nitrate from water by electroreduction and electrocoagulation. J. Hazard. Mater. 89, 83–94.
Krajangpan, S., Elorza Bermudez, J.J., Bezbaruah, A.N., Chisholm, B.J., Khan, E., 2008. Nitrate removal by entrapped zero-valent iron nanoparticles in calcium alginate. Water Sci. Technol. 58, 2215–2222.
Lacasa, E., Cañizares, P., Llanos, J., Rodrigo, M.A., 2011. Removal of nitrates by electrolysis in non-chloride media: effect of the anode material. Sep. Purif. Technol. 80, 592–599.
Loget, G., Kuhn, A., 2011. Shaping and exploring the micro- and nanoworld using bipolar electrochemistry. Anal. Bioanal. Chem. 400, 1691–1704.
Paidar, M., Bouzek, K., Bergmann, H., 2002. Influence of cell construction on the electrochemical reduction of nitrate. Chem. Eng. J. 85, 99–109.
Peel, J.W., Reddy, K.J., Sullivan, B.P., Bowen, J.M., 2003. Electrocatalytic reduction of nitrate in water. Water Res. 37, 2512–2519.
Probstein, R.F., Hicks, R.E., 1993. Removal of contaminants from soils by electric fields. Science 260, 498–503.
Zhang, Y., Li, Y., Li, J., Hu, L., Zheng, X., 2011. Enhanced removal of nitrate by a novel composite: nanoscale zero valent iron supported on pillared clay. Chem. Eng. J. 171, 526–531.
Zhou, M., Fu, W., Gu, H., Lei, L., 2007. Nitrate removal from groundwater by a novel three-dimensional electrode biofilm reactor. Electrochim. Acta 52, 6052–6059.